

---

## 3-6 Feed System

### 3-6-1 Configuration of the Feed System

UENO Kenji

Japanese Engineering Test Satellite VIII (ETS-VIII) is being developed and is scheduled to be launched into a geostationary Earth orbit to experimentally establish mobile communications and multimedia broadcasting services. Of the key technologies in ETS-VIII, we focus on an array-feed system for making multiple beams and illuminating large, deployable reflectors. Assembled array-feed system have been tested, and their ability to control RF signals in amplitude and phase has been confirmed satisfactorily. Based on measured array-feed radiation patterns, we have derived reasonable secondary radiation patterns of ETS-VIII S-band antennas. Environmental tests implemented to the feed units which are being placed outside the satellite body have certified sufficient durability in the launching period and space environment.

#### *Keywords*

Satellite communication, Engineering Test Satellite VIII, Multibeam antenna, Feed system, Feed unit

#### 1 Introduction

The mission of the ETS-VIII is to establish satellite-based mobile communication technology and multimedia broadcasting technology at an affordable price [1]. Specifically, the satellite's mission is to enable communication between handheld terminals through an onboard satellite switch and to permit reception of broadcast waves by small terminals within S-band (2.5-GHz) frequencies. Achievement of these objectives will require a multibeam antenna with a large-diameter deployable reflecting surface, a high-output transponder, an onboard switch, and small portable terminals. In this paper, we will discuss the technology relating to the onboard multibeam antenna.

Requirements for the antenna include high-gain multibeam capability, low sidelobes for the redundant use of frequencies, control of beam directionality, flexible control of beam shape, arbitrary power allotment among

transmitted beams, a high-output amplifier within a redundant configuration, and efficient radiation of RF power. To satisfy these requirements, a reflector antenna employing an array configuration for the primary radiator was adopted. This antenna functions in a manner similar to an antenna featuring an active phased array [2]; however, the design of the current configuration has yet to be finally established. We have determined the diameter of the antenna aperture, the setting position for the feeder array, and the spacing of array elements through calculation of the desired communications area of the ETS-VIII [3].

To construct an antenna-feed system that can withstand the space environment, we have focused on developing an array element, a solid state power amplifier, and a beam-forming network in the context of overall system design. We constructed the feed system by combining manufactured devices, confirming electrical operations, and experimentally verifying the antenna multibeam pattern. A num-

ber of tests involving heat, acoustics, and vibration were conducted to confirm that the feed system will function effectively in onboard satellite use, and an analytical model was designed to allow for future prediction of antenna performance.

The function and configuration of the feed system of the large deployable reflector on the ETS-VIII will be discussed in Section 2, the performance of the individual devices constituting the feed system will be described in Section 3, and Section 4 will address the electrical characteristics of the feed system, the radiation characteristics of the antenna, and the results of environmental testing.

## 2 Antenna and feed system

The appearance of the ETS-VIII is as shown in Fig.1. The satellite features two dishes of array-feeding reflector antennas; one for transmission and one for reception. This reflecting surface forms an offset paraboloidal reflecting surface made of metal mesh, with an aperture interior diameter of 13 m and an outer diameter of 17 m [4]. The primary radiator of the active phased array illuminates the reflector, and is arranged not at the focal position of the reflector, but at a point away from the focal position, slightly toward the reflecting surface, i.e., in an off-focus position. This arrangement is chosen in order to enable operations similar to those performed by a normal

phased-array antenna that does not feature a reflecting surface [5], as this arrangement allows for an expanded beamwidth in a secondary radiation pattern (referred to as a component beam) when the individual array elements direct their beams toward the reflector. Consequently, this arrangement allows for superposition of component beams, each of which corresponds to a single array element.

The feed system is composed of primary array radiators, amplifiers, beam-forming networks, and other elements, and is configured as shown in Fig.2. The dotted lines in the figure show the various subsystems (with the exception of the feed system). In the figure, a transmission feed unit (Tx unit) and a reception feed unit (Rx unit) are shown combined within the feed system; this combination of devices must be arranged near the primary array radiator. The devices are assembled in a single enclosure installed on the top of the antenna tower; this equipment must feature robust environmental resistance. The Tx unit consists of array elements, filters, and solid state power amplifiers (SSPAs). The Rx unit consists of array elements, filters, and low-noise amplifiers (LNAs).

The beam-forming network excites amplitude and phase for each array element, shaping the RF beam signals into predetermined radiation patterns. Although each beam port features two beam-forming networks (two for transmission and two for reception), only one

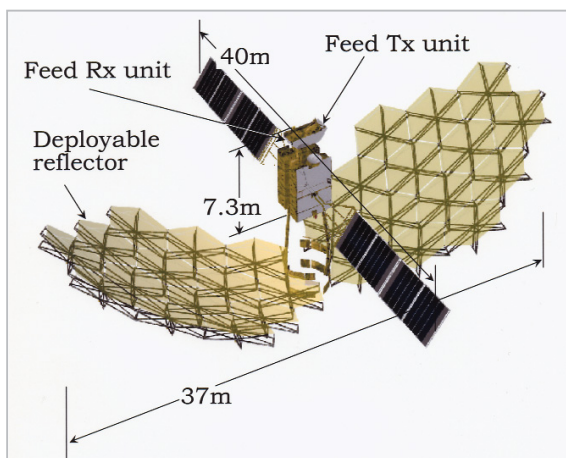


**Fig. 1** Appearance of the ETS-VIII

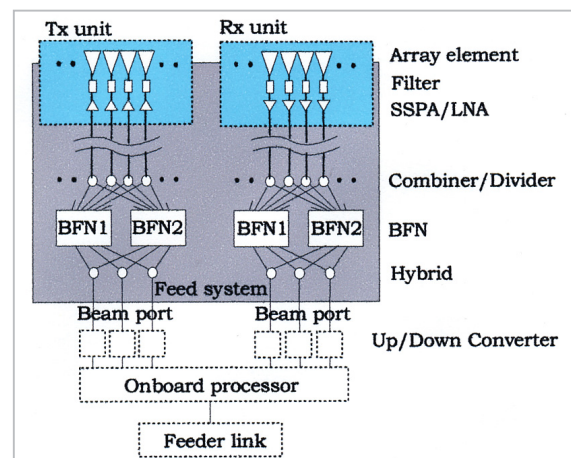


**Fig. 2** Configuration of feed system

transmission network and one receiving network are employed in actual operation. Moreover, the input terminals and output terminals of the two beam-forming networks are connected to hybrids, resulting in continuous in-parallel connection. The beam-forming networks and the hybrids are incorporated into the satellite structure.

### 3 Devices constituting feed system

#### 3.1 Array feed element

The transmission feed unit (Tx unit) is as shown in Fig.3. A planar array consisting of thirty-one micro-strip antennas [6] equipped with cups (metal cylinders) is disposed across a single surface. Each micro-strip antenna, acting as an array element, is affixed with a hybrid substrate layer (on the reverse side of the antenna), and radiates a circularly polarized wave by a dual-point feeding method. Moreover, output feed is performed via a non-contact feeding method employing slot connection, designed to suppress passive intermodulation (PIM) and to improve overall functional efficiency. Experimental verification of the metal cylinder led to a diameter specification of 120 mm, with height set to 40 mm. The transmitting frequency was set at 2,500 to 2,505 MHz for communications and 2,535 to 2,540 MHz for broadcasting, and the receiving frequency was set at 2,655 to 2,660

MHz.

Characteristics of this micro-strip cup antenna are as follows: bandwidth is 4%, gain is 8.9 to 9.8 dBi (for transmission) and 10.3 to 10.8 dBi (for reception), half power beamwidth is 60 degrees, axial ratio is 1.5 dB or less, mutual coupling with the adjacent array element is  $-40$  dB or less, and weight is 180 g.

#### 3.2 Filter

A transmission filter is inserted between the solid-state power amplifier and the array element to suppress spurious and intermodulation waves. In particular, its main purpose is to limit leakage to the received frequency band. The filter is of the dielectric resonator type, features insertion loss of 0.3 dB or less, attenuation of 70 dB or more in the received frequency band, power endurance of 40 W or more, installation area of  $100 \times 100$  mm<sup>2</sup>, and a weight of 300 g. A reception filter is provided to prevent high-power transmitted waves from entering the low-noise amplifier via the array elements and causing interference. Fig.4 shows a group of reception filters arranged in the reception feed unit (Rx unit). The employed filter is of the coax resonator type, featuring insertion loss of 0.4 dB or less, attenuation of 70 dB or more in the transmitting frequency band (for communications), an installation area of  $180 \times 60$  mm<sup>2</sup>, and a weight of 190 g.

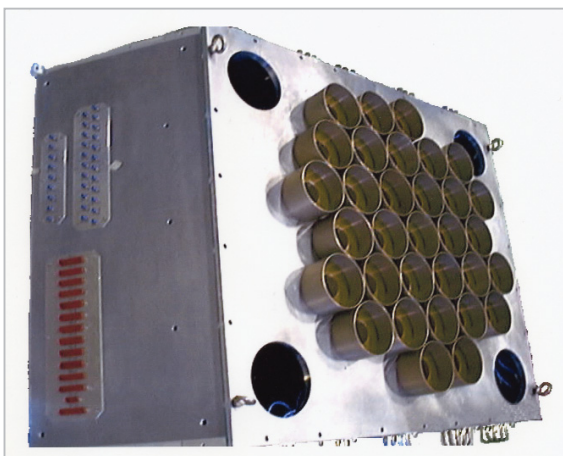


**Fig.3** Appearance of Tx unit



**Fig.4** Filter arrangement in Rx unit

### 3.3 Solid-state power amplifier

The primary array radiator of the transmitting antenna was designed with a series of fixed excitation values for amplitude; only phase is freely controlled in beam formation. This specification was selected based on the concept of allotting an appropriate power amplifier to each array element in order to avoid unnecessary power consumption and to reduce weight. This option was selected over the allotment of high-output power amplifiers to all of the array elements, which would have provided more flexible control of excitation amplitude.

The excitation amplitude of the array element is illustrated in Fig.5; this value can be set to 0, -3, or -6 dB. Two types of solid-state power amplifier are employed, featuring 10-W and 20-W output, respectively. Twenty-three of the 10-W amplifiers and eight of the 20-W amplifiers are employed. The three excitation amplitude values and the input level of a given amplifier to one of two levels are set for this configuration. These amplifiers are designed to ensure gain and phase stability at different input levels and variable environmental temperatures [7].

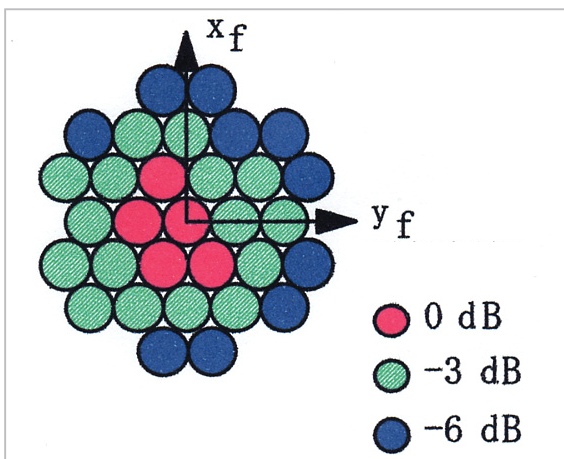


Fig.5 Excitation amplitude of array element

Fig.6 shows the 10-W solid state power amplifier, featuring gain of  $55.0 \pm 0.5$  dB, temperature-dependent gain deviation of 0.8 dBp-p or less (for a temperature variation from 0°C to 50°C), gain flatness of 0.15 dBp-p/5 MHz or less, temperature-dependent phase deviation of 19 degp-p or less, phase flatness of 13 degp-p/5 MHz, a noise/power ratio of 17.4 dB or more, an installation area of  $260 \times 60$  mm<sup>2</sup>, and a weight of 660 g.

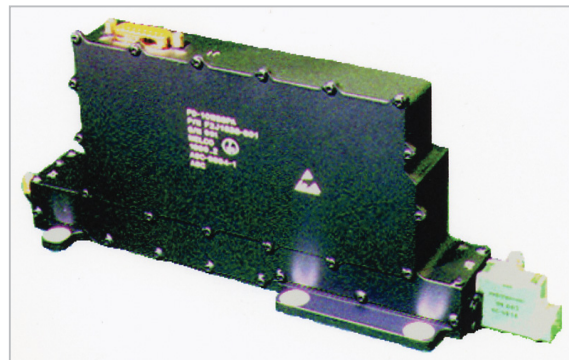


Fig.6 10-W solid-state power amplifier

The 20-W solid state power amplifier features gain of  $57.9 \pm 0.4$  dB, gain flatness of 0.14 dBp-p/5 MHz or less, phase flatness of 2 degp-p/5 MHz, a noise/power ratio of 17.2 dB or more, an installation area of  $220 \times 210$  mm<sup>2</sup>, and a weight of 2,500 g.

The 20-W solid state power amplifier features gain of  $57.9 \pm 0.4$  dB, gain flatness of 0.14 dBp-p/5 MHz or less, phase flatness of 2 degp-p/5 MHz, a noise/power ratio of 17.2 dB or more, an installation area of  $220 \times 210$  mm<sup>2</sup>, and a weight of 2,500 g.

### 3.4 Low-noise amplifier

Fig.7 shows the low-noise amplifier, a low-power component, arranged within the Rx unit. For the primary array radiator of the receiving antenna, independent excitation amplitude is given to each beam, as fixing the excitation amplitude (as in the transmitting antenna) would not reduce power consumption. Only one type of low-noise amplifier is employed, featuring gain of  $44.8 \pm 0.5$  dB, gain flatness of 0.5 dBp-p/5 MHz or less, phase flatness of 0.6 degp-p/5 MHz, phase tracking of 5 degp-p, a noise factor of 1.4 dB

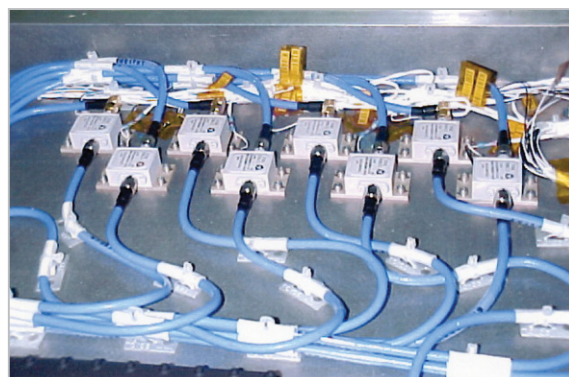
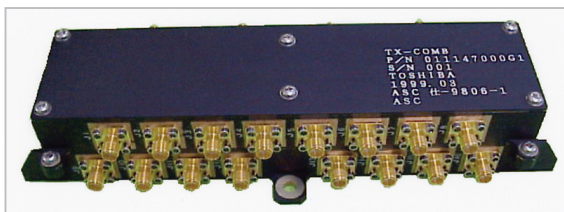


Fig.7 Low-noise amplifier within Rx unit

or less, an installation area of  $42 \times 40 \text{ mm}^2$ , and a weight of 50 g.

### 3.5 Hybrid

Since this feed system includes two beam-forming networks, three hybrids are arranged on the beam port side (the side to be connected to the transponder) and thirty-one hybrids are arranged on the element port side (the side to be connected to the array elements). On the element port side, eight hybrids are housed in two tiers within a single housing in order to save installation space. The combined hybrids for transmission are referred to as “combiners” and those for reception are referred to as “dividers.” Fig.8 shows the appearance of the hybrid. The hybrid features insertion loss of 3.5 dB or less, passing amplitude error of 0.2 dBp-p or less, passing phase error of 5 degp-p, an installation area of  $200 \times 70 \text{ mm}^2$ , and a weight of 360 g.



**Fig.8** Appearance of hybrid

## 4 Overall characteristics of feed system

### 4.1 Electrical characteristics

The devices described in Section 3 have been assembled within the feed system. A partial view of this system within the satellite structure is shown in Fig.9. Electrical testing of the feed system confirmed that the formed beam is of the required amplitude and phase with the given excitation values; i.e., the formation of a predetermined beam was confirmed within the beam-forming network and within the field of radiation in the vicinity of each array element under measurement [8]. Accumulated errors in gain, loss, and phase caused by the array elements, the amplifiers, and connection cables are all corrected by the

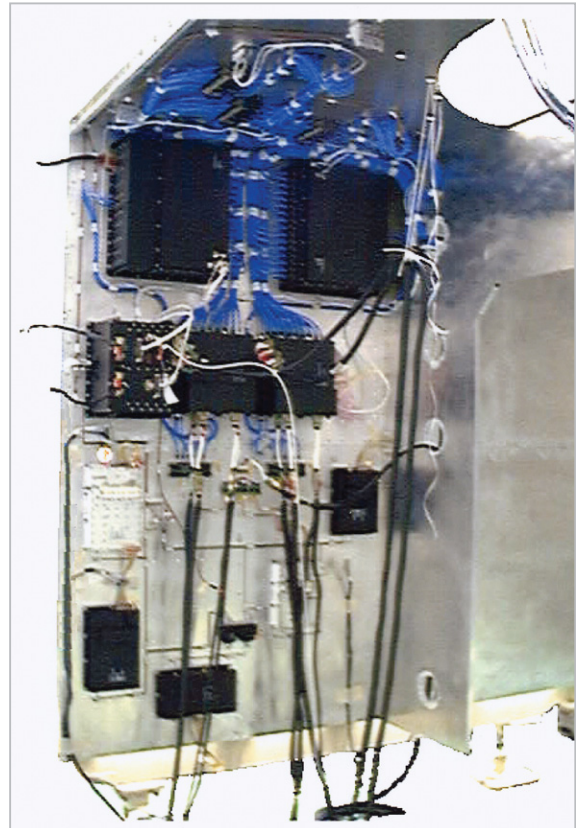


**Fig.9** Feed system within the satellite structure

beam-forming network, thus satisfying the requirements applicable to amplitude and phase of the individual beams. Actual final residual error will depend on the precision of control and measurement errors within the beam-forming network.

Fig.10 shows both the amplitude and phase measured in the vicinity of the array elements and the required values. Fig.10(a) corresponds to transmission beam #1 (directed to the Kyushu area), and Fig.10(b) corresponds to reception beam #1. Deviations from required values for all beams were 0.5 dB rms and 4.2 deg rms, both for transmission and reception. These results satisfy the initial required values of 0.6 dB and 7.3 deg. All of the power amplifiers are to be used in the linear region, and the total of their RF outputs in this configuration reached 355 W. The overall feed system weighs 235 kg.

### 4.2 Radiation characteristics

The radiation pattern of the primary array

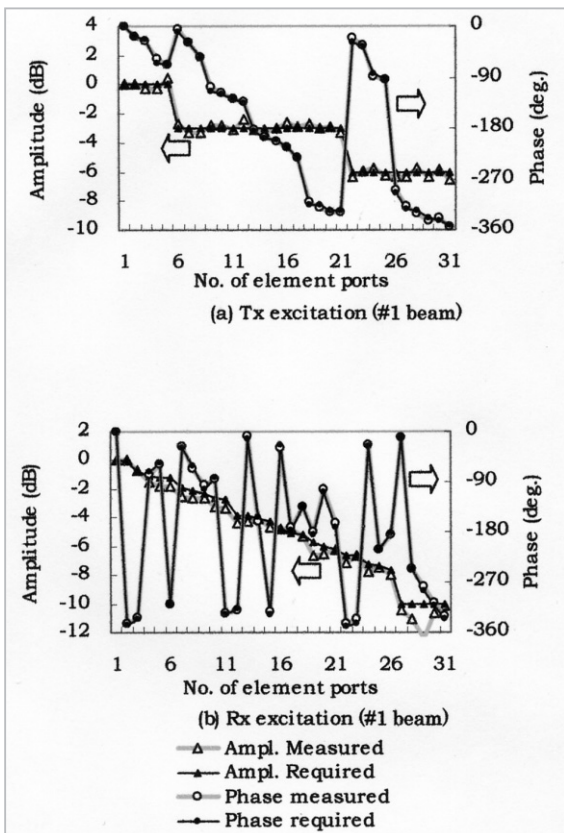


**Fig. 10** Measured values and required values of excitation amplitude and phase

radiator was measured with a planar near-field measuring instrument. This radiation pattern is used to evaluate the radiation pattern of the overall antenna, including the reflector. Fig.11 shows the radiation pattern of the pri-

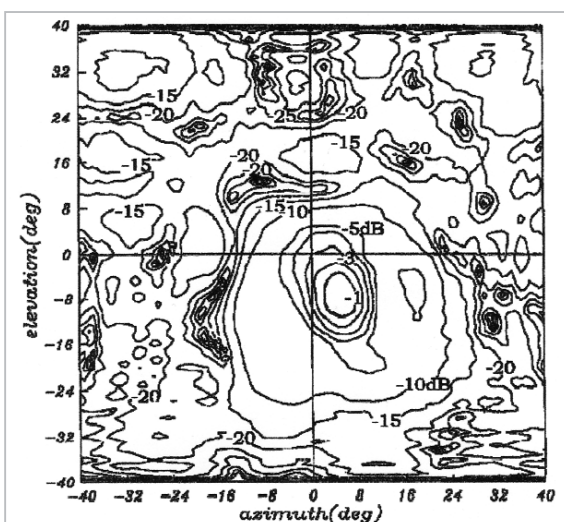


**Fig. 11** Feed system radiation pattern in transmission (beam #1)

mary array radiator of the beam #1 from the transmitting antenna, drawn from the measured results for individual beams and radiation patterns. The axial ratio of the antenna was also measured together with pattern measurement; the value was determined to be 1.5 dB or less.

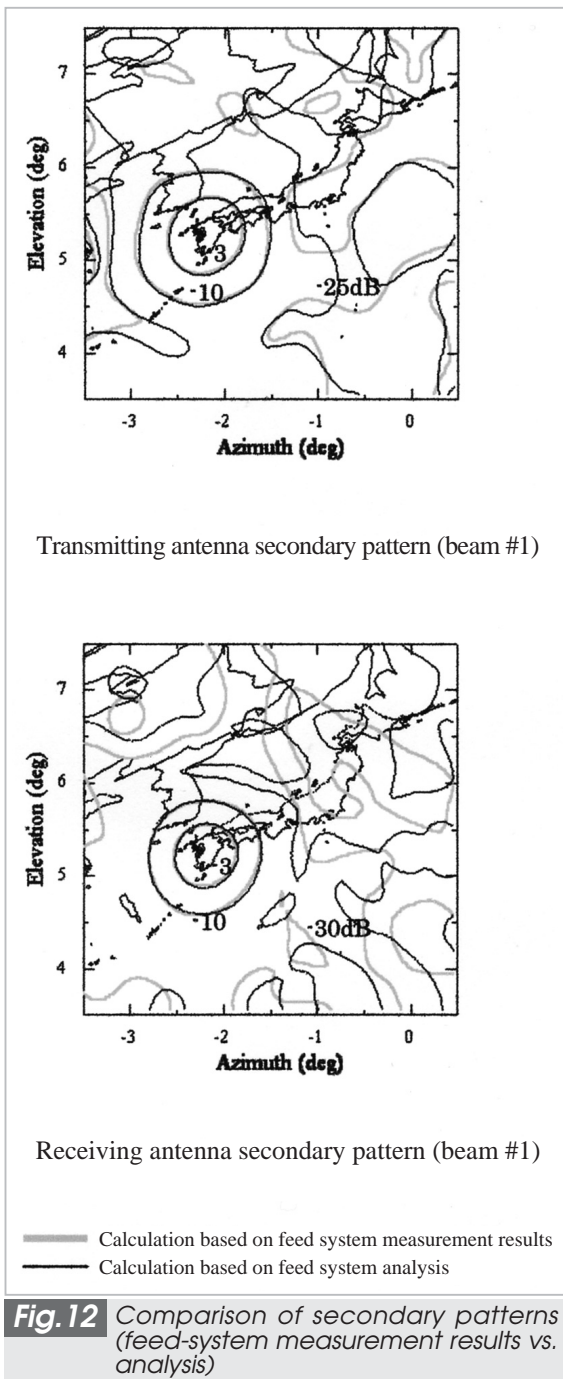
The procedure for obtaining the radiation pattern of the overall antenna (including the reflector) is as follows: the aperture distribution on the primary array radiator is obtained by a reverse projection of near-field data processing; the RF current induced on the reflecting surface is then calculated based on this aperture distribution, and the radiation pattern is determined through integration of the radiation field. The reflecting surface is composed of fourteen hexagonal modules featuring metal mesh surfaces. The radiation pattern is analyzed under the assumption that the reflecting plane is a conducting metallic plane, taking gaps between modules into consideration.

Fig.12 shows a comparison between the secondary radiation pattern obtained through the application of this method to the measured results of the primary radiator and the secondary pattern obtained by theoretical analysis of the primary radiator. The figure indicates that these patterns agree for most elements of the main lobe and the sidelobes; however, a discrepancy appears in the  $-25$  dB contour (transmission) or the  $-30$  dB contour (reception). This discrepancy is attributed to residual errors in the excitation amplitude and phase of the primary array radiator and to analytical error in near-field measurement.

Summarizing the conclusions drawn from these secondary antenna radiation patterns, we can confirm that the isolation between a beam and the nearest beam using the same frequency is 19 dB or more in transmission and 25 dB or more in reception. Moreover, the axial ratios of all beams were 2 dB or less for both transmission and reception.

Measurement of the near-field radiation characteristics of the antenna using a part of the deployed reflecting surface and the feed system was also conducted, confirming the

validity of the analytical models of the deployed reflecting surface [9].



### 4.3 Thermal characteristics

Since the Tx unit and the Rx unit are installed on the east/west panels of the antenna tower on the satellite structure, these units must be subject to thermal control independent of the satellite system. In conventional geostationary satellites, heat-generating

devices such as SSPAs were fixed on the north/south mission panels to allow heat to dissipate directly from the radiating surfaces. However, in a phased-array feed system, SSPAs must be installed in the vicinity of the array elements in order to reduce SSPA output loss. The SSPA installation area is further limited due to the structure of the antenna fairing and the antenna tower. Thus, a total of 31 SSPAs must be installed in a high-density configuration. As a result, up to 1.4 kW of heat energy is generated within the Tx unit.

It was determined that a heat pipe would be used to transport heat to a radiating panel mounted on the north/south panels of the antenna tower for dissipation. Fig.13 shows the SSPA arrangement and the disposition of the heat pipes in the Tx unit.

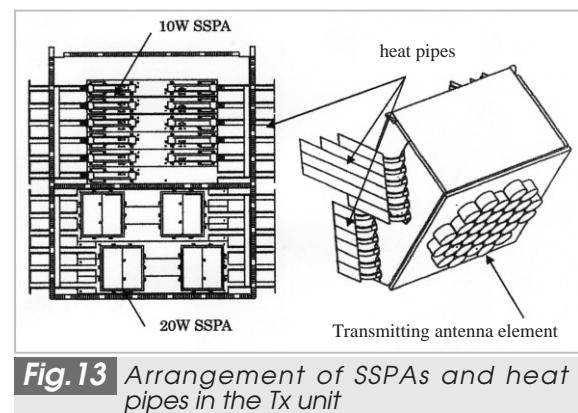
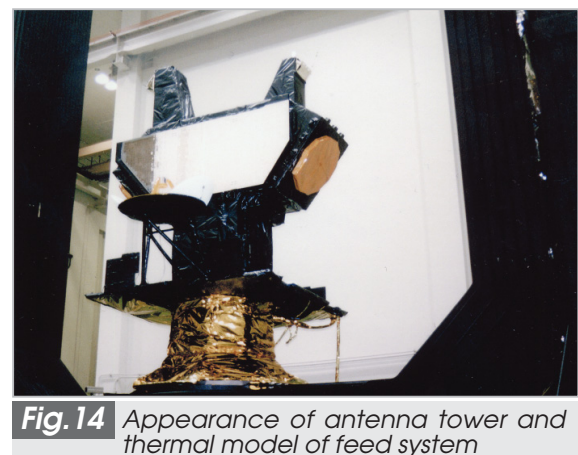


Fig.14 is a photograph of the antenna tower with the feed-unit thermal model installed (the thermal model will be modified to a flight model following completion of the



thermal test). The Tx unit is affixed to the east panel of the antenna tower (right-hand side of the figure); heat generated within the feed unit is dissipated from a radiating panel (center in the figure) of the north/south panels of the antenna tower. The primary array radiator is insulated from the interior of the feed unit, and is thermally controlled independently, with the outer surface of the radiator covered with Tedra Kapton film.

The Rx unit is installed on the west panel of the antenna tower (left-hand side of the figure); heat generated within the feed unit is dissipated from a radiating surface on the upper side of the unit. The primary array radiator is insulated from the interior of the unit as with the Tx unit, and is thermally controlled independently, with the outer surface of the radiator covered with Tedra Kapton film.

Thermal balance testing was conducted in a space chamber after combining the antenna tower, an antenna for a highly precise time reference apparatus, an antenna for feeder link, and an earth head panel dummy [10]. Including the earth head panel in the testing configuration enables verification of the thermal design of the feed system, at the same time confirming the performance of the thermal interface between the feed system and the overall system.

For the test, four stationary cases (winter solstice, summer solstice, equinox<sup>1</sup>, and equinox<sup>2</sup>) and two nonstationary cases (eclipse and orbital transfer) were evaluated. External thermal input was generated by a solar simulator. Evaluation of the stationary cases was intended to provide data for correlation with the results of the thermal mathematical model, while experimentation involving anticipated thermal environments in orbit was designed to yield thermal balance data. The nonstationary experiments were structured to acquire temperature data in order to evaluate expected thermal behavior during eclipse or orbital transfer.

Since the measured test results differed from the predicted temperatures for the array element, the LNA, and the reception filter, the

thermal mathematical model has been corrected accordingly. Consequently, in post-test analysis using a model subject to such correction, the difference between the predicted temperature and the measured temperature was reduced to within 10°C for all test cases. The corrected model was thus shown to provide sufficient accuracy in the prediction of orbital temperatures. In particular, for the key SSPA components, temperatures can be predicted within 5°C. We then performed further orbital temperature analysis using the corrected model, in the process confirming that all onboard devices can be maintained within the predetermined ranges from launch through the final mission stages. Table 1 shows the results of analysis.

**Table 1** Results of orbital temperature prediction

	Specific allowable temperature in operation (°C)	Specific allowable temperature in non-operation (°C)	Predicted temperature (°C)
SSPA	-10~55	-30~60	-13~45
Tx-FIL	-35~85	-35~85	-20~38
Tx array element	-100~110	-100~110	-80~93
LNA	-20~60	-30~60	-14~44
Rx-FIL	-35~85	-35~85	-20~36
Rx array element	-100~100	-100~100	-77~63

#### 4.4 Acoustic test characteristics

The acoustic test is conducted to verify that the feed units can withstand acoustic vibration during launch. Fig.15 is a photograph of the acoustic testing apparatus for the structural model of the feed system. The results of these tests clarify the following three points:

- (1) Visual inspection of the Tx unit and the Rx unit revealed no abnormalities such as deformation of the test specimen. As no problems were seen with the units in this case, we have successfully demonstrated that the structural model of the feed system mounted on the tower is capable of withstanding acoustic qualification test levels.
- (2) Although the PSD (Power Spectrum Density) levels of the array elements, the filters, the 10-W SSPAs, and LNAs revealed that the effects of random vibration were greater than anticipated, examination of

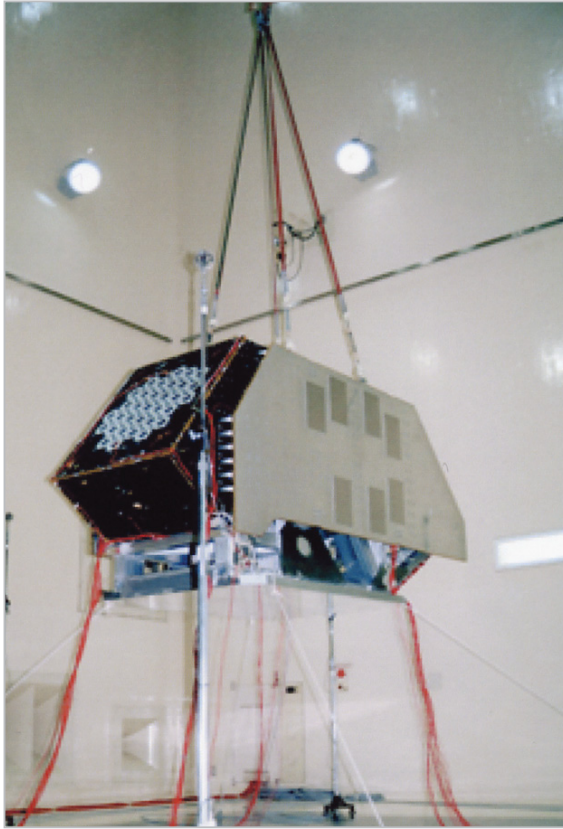


**Fig. 15** Experimental configuration of acoustic testing of structural feed-unit model

the individual devices confirmed that this excess vibration presented no problems in the given frequency bands.

- (3) The test jig presented no problems in use, with an effective acoustic response as low as 2 Grms or less, confirming that this test jig may be successfully applied to proto-flight testing (PFT).

#### 4.5 Vibration test characteristics

The vibration test is conducted to verify that the feed units can withstand the vibration environment at the time of launch. Fig.16 is a photograph of the experimental configuration of vibration testing of the structural feed-unit model. Results of these tests have indicated the following.

- (1) The structural feed-unit model can withstand the sinusoidal vibration environment.
- (2) The feed unit structural model satisfies the natural frequency requirement of 50 Hz or higher.

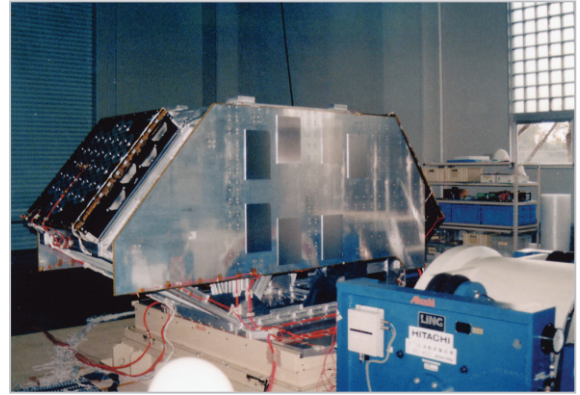


**Fig. 16** Configuration of vibration testing of the feed-unit structural model

- (3) The sinusoidal vibration characteristics of the devices comprising the onboard feed unit structural model were confirmed.
- (4) Based on the results of the sinusoidal vibration test, the structural analysis model was modified so that the natural frequency of the model agreed with test results within several Hz.
- (5) There is no resonance point at 150 Hz or less for the Z-axis of the test jig. Although resonance points are noted at 100 Hz or higher for the X-axis and the Y-axis, acceleration response is high even at the rising slope of the resonance point. These results have established that controlling the test jig response acceleration using a limiter will allow for the use of the test jig (as well as the vibration test facility) in connection with PFT.

## 5 Concluding remarks

In the development of the ETS-VIII, we have focused on and provided a detailed analysis of a feed system featuring a primary array radiator. This system consists of thirty-one array elements feeding a large deployable antenna reflecting surface, permitting effective multibeam formation. We have completed manufacture of array elements, filters, solid-state power amplifiers, beam-forming networks, hybrids, and the remaining component devices of the feed system, and have confirmed that these devices can withstand use in the satellite in terms of electrical characteris-

tics and environmental resistance. We conducted testing of the overall feed system, confirming that RF signal control in multibeam formation can be performed with sufficient accuracy. Measurement of the radiation pattern of the feed system revealed that the multibeam pattern of the overall antenna was in accordance with design. Moreover, environ-

mental testing (thermal, acoustic, and vibration testing) has confirmed that the feed system will be able to function aboard the satellite, in the process permitting modification of the analytic model. Data thus obtained will in turn facilitate future testing and improve the prediction of system performance.

## References

- 1 Y. Kawakami, S. Yoshimoto, Y. Matsumoto, T. Ohira, and N. Hamamoto, "S-band mobile satellite communications and sound broadcasting systems in ETS-VIII", 21st Int. Symp. on Space Tech. and Science, 98-h-02, pp.1362-1367, May 1998.
- 2 R. Lo. Forti, "Advanced imaging antenna for satellite application at L-band", IEEE AP-S Int. Symp., pp.1618-1621, 1989.
- 3 K. Tokunaga, H. Tsunoda, H. Shoki, and M. Okumura, "Design optimization of phased-array-fed reflector antennas for mobile communication satellites", AIAA Journal of Spacecraft and Rockets, Vol.36, No.1, pp.105-108, Jan.-Feb. 1999.
- 4 K. Yonezawa, M. Homma, S. Yoshimoto, S. Hama, T. Ohira, N. Natori, and Y. Tsutsumi, "Outline of Engineering Test Satellite-VIII (ETS-VIII)", 21st Int. Symp. on Space Tech. and Science, 98-h-01V, pp.1356-1361, May 1998.
- 5 K. Ueno, "Multibeam antenna using a phased array fed reflector", IEEE AP-S Int. Symp., pp.840-843, 1997.
- 6 M. Tanaka, "Effect of the height and diameter of the cup on cup microstrip antennas", IEICE Trans. Commun., Vol.E81-B, No.8, Aug. 1998.
- 7 H. Ishida, Y. Kawakami, H. Hirose, and M. Shigaki, "Solid-state power amplifiers for the Japanese Engineering Test Satellite-VIII", Sixth Int. Mobile Satellite Conf., pp.258-261, June 1999.
- 8 M. Atobe, K. Ueno, M. Okumura, K. Tokunaga, and Y. Yamasa, "Development test results of phased array antenna feed for the Engineering Test Satellite-VIII", IEICE National Conv., B-3-29, p.285, Mar. 2000.
- 9 K.Ueno, M. Atobe, A. Miyasaka, T. Orikasa, and M. Okumura, "Ground test of array-fed reflector antennas for ETS-VIII", IEICE Tech. Rept., AP2000-155, Jan. 2001.
- 10 A. Tanaka, A. Saito, M. Okumura, J. Asaga, M. Atobe, K. Ueno, and A. Tsujihata, "Thermal Balance test for large deployable antenna feed of the Engineering Test Satellite-VIII", 44th Space Science Tech. Conv., 00-1F15, Oct. 2000.



**UENO Kenji, Dr. Eng.**

*Professor, Department of Information Network Engineering, Hokkaido Institute of Technology*

*Satellite Communication and Antenna Engineering*